Optimizing parameters in an atmospheric general circulation model.

C. A. Severijns[1] and W. Hazeleger

Royal Netherlands Meteorological Institute

P.O. Box 201, 3730 AE De Bilt, Netherlands

2 August 2004

[1]Corresponding author: `c.severijns@knmi.nl`

Abstract

We describe an efficient method to optimize the parameter values of the subgrid parameterizations of an Atmospheric General Circulation Model. The method is based on the downhill simplex minimization of a cost function computed from the difference between simulated and observed fields. We use it to find optimal values of the radiation and cloud related parameters. The model error is reduced significantly within a limited number of iterations (about 250) of short integrations (5 years). The method appears to be robust and finds the global minimum of the cost function. The radiation budget of the model improves considerably without violating the already well-simulated general circulation. Different aspects of the general circulation, such as the Hadley and Walker Cells improve, although they are not incorporated into the cost function. We conclude that the method can be used to efficiently determine optimal parameters for general circulation models even when the model behavior has a strong nonlinear dependence on these parameters.

1 Introduction

Studies on climate and climate change rely partially on simulations with numerical models of the different components of the climate system. Elaborate coupled ocean/atmosphere models are based on the primitive equations and a set of parameterizations that represent the subgrid scale processes. Although numerical models are very useful to study the climate system, biases occur in these models. Well known biases are the occurrence of a Intertropical Convergence Zone (ITCZ) to the north and to the south of the equator, while the ITCZ stays to the north of the equator in reality (see Davey et al. 2002). Other shortcomings are the lack of stratiform clouds in the east of the subtropical ocean basins and the bad simulation of tropical Atlantic zonal temperature gradients. Also dominant modes of variability such as the El Niño Southern Oscillation (ENSO) are not well simulated by the coupled models (Latif et al. 2001). Furthermore, many models don't have a closed energy budget and need flux correction to avoid drift. Many of the shortcomings of the models can be attributed to the parameterization schemes that are used and the uncertainty in their parameters. Changes in the parameterizations can have a large effect on the simulated mean state and variability (e.g. Terray 1998).

The procedure to find the optimal set of parameters in a model is usually referred to as tuning. The tuning of a nonlinear system such as an atmospheric general circulation model (AGCM) is typically done manually by trial and error and is a labor intensive work. There are many parameters (typically between 10 and 100) that need to be considered in the optimization process. In addition, the nonlinear nature of the system makes it difficult

to predict what the result will be when the values of several parameters are changed simultaneously. Therefore, a systematic approach using a minimization routine to find the best estimate of a (sub)set of the parameters would be useful. Several authors have applied an automatic optimization procedure to idealized models with relatively few parameters with reasonable success. For instance, Sennéchael et al. (1994) optimize a sea surface temperature (SST) model for the tropical Atlantic using an adaptive inverse model. They succeed in improving the annual mean SST of their model. However, the seasonal and interannual variability is not improved. Ensemble Kalman filter (EnKF) based data assimilation is a well-known method for improving the results of numerical weather prediction models (e.g. Wahba et al. 1995). This method has been applied to parameter estimation of a 3D frictional geostrophic ocean model coupled to a 2D energy moisture balance atmosphere and thermodynamic sea ice model by Annan et al. (in press). They optimized this model to a synthetic truth. The EnKF worked well in this case because the model had hardly any internal temporal variability (Annan and Hargreaves 2004). The EnKF and other data assimilation methods were developed for the optimization of large numbers of parameters ($> O(10^3)$) and is based on a linearization of the problem. As result, the method is not well suited for problems with a small number of parameters where it is possible to deal with nonlinearities directly. Other methods, such as the downhill simplex method used here, might prove more efficient in such cases.

In this paper we illustrate the use of the downhill simplex method by improving the climatology of an AGCM. We describe the optimization method in section 2 and present our results in section 3. This is followed by a discussion and conclusions in section 4. We

4

illustrate the method with an AGCM, but it can be easily expanded for use in a coupled climate model.

2 Method

The model that we are concerned with in this paper is called SpeedO (for Speedy-Ocean). The atmospheric component, Speedy, is a primitive equation model with seven layers and truncated at wavenumber 30 with a triangular filter. It uses a set of simplified parameterization schemes based on the same principles adopted in state-of-the-art AGCMs. The five-layer version of Speedy is described by Molteni (2003). The 7-layer version has an improved climatology and is described in Hazeleger et al. (2003) and Bracco et al. (2003). In our optimization experiments, surface temperature, albedo, and soil water availability are prescribed.

We will focus on the radiation budget at the top of the atmosphere (TOA) and at the surface, and aspects of the large-scale circulation. A correct simulation of the radiation balance is necessary to avoid drift in coupled models. It is to be expected that the parameterization of radiation, clouds and convection are important for the simulation of the radiation balance and the large-scale circulation. Therefore, we will optimize the parameters of the parameterizations of these processes.

In order to improve our model we want to close the energy budget at the bottom boundary of the atmosphere and reduce the error with respect to a reference dataset consisting of a 12 month climatology of TOA and surface fluxes, cloud cover, zonal mean

precipitation, and specific humidity at 925 hPa. We decided to use the corrected Da Silva data (Da Silva et al. 1994) at the sea surface and to exclude the land areas. For the other fields we use the National Centers of Environmental Prediction Reanalysis data (Kalnay et al. 1997, henceforth Reanalysis), CPC merged analysis of precipitation (CMAP) (Xie and Arkin 1996) and cloud cover data from Oberhuber (1988). Note that the surface heat flux balance is not closed in the Reanalysis data, hence the choice for the Da Silva data for the surface fluxes. The complete list of data we have selected is shown in table 1.

The function that we want to optimize is the χ^2-norm of the errors of the model's climatology with respect to the reference data

$$\chi^2 \;=\; \sum_F \left(\frac{1}{N^F} \sum_{i=1}^{N^F} \left(\frac{x_i^F - x_0^F}{\sigma^F} \right)^2 \right) \tag{1}$$

Here the index F runs over all fields of the reference dataset and the index i over the points in each field of the dataset. We normalize the deviation from observational data with an error estimate σ^F. The contribution for each field is divided by the number of grid points, N^F, to compensate for the fact that some fields are masked. Since our main interest is in improving the climatology of Speedy, it is not necessary to have precise knowledge about the errors at each data point. What matters is that the ratio of the errors in the data fields are represented correctly. Therefore, we use values of σ^F that are reasonable representations of the errors in the data. Our values of σ^F over sea are similar to those given in Taylor (2000). The values of σ^F are listed in table 1 as well.

Due to its simplified physics parameterizations and resolution of 3.75°, Speedy is fast

6

compared to state-of-the-art AGCMs. The number of tunable parameters in the radiation, cloud and convection schemes of Speedy is about twenty. Given this number of parameters we expect that $O(10^2)$ iterations are required. With current computing power, running Speedy for 10^3 years requires about three weeks of computer time. This means that the length of individual runs will not be long enough to suppress sampling variability. Therefore the optimization routine should not be sensitive to noise. This excludes any routine that depends on the availability of accurate values for the gradient of the function being optimized. For many of the parameters, there are physical constraints on the value. It should be possible to take such constraints into account in the optimization process. Although it is not a very efficient method, the downhill simplex method (Press et al. 1992) satisfies these criteria. In this method a set of $d+1$ points $\{\vec{p}_i\}$ — the vertexes of a simplex in d-dimensional parameter space — is modified in order to locate the minimum of a cost function $C(\vec{x})$ which in our case is given by χ^2 defined in equation 1. The values of the cost function on these points $\{C_i\} = \{C(\vec{p}_i)\}$ are used to determine a new point $\vec{p}$ on which $C(\vec{x})$ is evaluated. When $C(\vec{p}) < \max_i\{C_i\}$, $\vec{p}$ replaces the point with the largest cost function value in $\{\vec{p}_i\}$. This iterative process continues until convergence is obtained, i.e., until

$$\frac{\max_i\{C_i\} - \min_i\{C_i\}}{\max_i\{C_i\}} \leq \epsilon \qquad (2)$$

with ϵ the required relative accuracy. This condition implies that the actual minimum is located inside the volume bounded by the simplex $\{\vec{p}_i\}$. While searching, new points are selected by expanding or shrinking one or more of the vertexes of the simplex $\{\vec{p}_i\}$ by a

constant factor. Together with the fact that $\vec{p}$ only replaces a point in $\{\vec{p}_i\}$ when $\max_i \{C_i\}$ decreases, this ensures that the method is not sensitive to noise in the cost function. The accuracy ϵ with which the minimum value of the cost function $C(\vec{x})$ and the optimal value of the parameters $\{\vec{p}_i\}$ can be determined is limited by the noise in the simulated data. The implementation of the downhill simplex method that we have used is the routine amoeba described in Press et al. (1992).

In the following section we will illustrate this optimization procedure by applying it to SpeedO and comparing results from the initial and optimized model. We will focus on two important aspects of the global climate system: the global energy budget (which should be closed) and associated fields such as cloudiness, and the large-scale circulation.

3   Results

Since the radiation related climatology data from Speedy differ most from Reanalysis data we optimized the 14 parameters of the short and long wave radiation and cloud parameterizations. Each iteration the model was run for 5 years and a 12 month climatology was computed from the data of years 2 to 5. The first year was omitted from the analysis to allow the model to spin up. Although the sampling time is relatively short given the internal variability of the atmosphere, the small variations of χ^2 at the end of the optimization process shows that it is sufficiently long. The optimum parameter values were found after 250 iterations which corresponds to running the model for a total of 1250 years. Figure 1a shows that the value of χ^2 changed from 6.0 to approximately 4.2. Note that χ^2 does

8

not decrease monotonically because the cost function values that were rejected during the optimization are also plotted. Some of the optimum parameter values differ significantly from their initial values, in particular the cloud related absorption coefficients for short and long wave radiation. The values of some parameters as a function of χ^2 are shown in Figure 1b. The fact that the values of χ^2 and all parameters converge, indicates that the optimum parameter values were found. To compare the model results before and after optimization two hindcast runs were done using Reanalysis data from 1961 to 2000 for the SST. On land no anomalies were applied.

3.1 The Global Energy Budget

In table 2 the global mean values of TOA and surface energy budgets are shown. There are noticeable improvements in the short and long wave radiation budgets and the global mean energy deficit over the ocean. Both annual mean TOA solar radiation (TSR) and surface solar radiation (SSR) are closer to the corresponding reference data. Figure 2 shows the annual mean SSR and the difference with Da Silva data for the model using the initial and optimal parameter values. Clearly, the SSR improved everywhere except for the stratus areas in the eastern part of the ocean basins. Here the errors remain large (50 W m^{-2}) because the model is not able to produce sufficient cloud cover in these areas. This is not the result of the choice of parameters but indicates the failure of the current parameterization scheme. The SSR changes are mainly caused by the changes in cloud cover. The error in the cloud cover has been reduced from 20 to 10 percent over ocean

9

areas except for the areas covered by stratus clouds.

The global time mean surface and TOA long wave radiation fluxes have also improved but are not as close to the climatological values as the short wave fluxes. The surface long wave radiation (SLR) has increased by about 10 W m^{-2} over all ocean areas. However, the difference in these fields between the original model and Da Silva datasets indicates that an increase of about 30 W m^{-2} between 40°S and 40°N and decrease by the same amount elsewhere is required. This suggests that absorption of long wave radiation by water vapor which is mostly concentrated in this area is too strong in the model. Since none of the optimal parameter values is close to its limiting values it is most likely the result of the long wave radiation scheme used in the model.

The global time mean values of latent heat flux (LHF) and sensible heat flux (SHF) have not changed significantly but their spatial distribution over sea has (see Figure 3). Both are reduced by up to 10 W m^{-2} between 40°S and 40°N. Elsewhere changes in these fluxes over sea are small. The net heat flux over sea (NHFS) decreased by more than a factor of two but the net heat flux over land (NHFL) did not improve. This is due to the fact that the surface flux terms in the cost function given by equation 1 were computed with respect to oceanic Da Silva data so that land areas were not optimized.

3.2 The Large-Scale Circulation

In section 3.1 we discussed the improvement in the radiation fields. These fields were included in the cost function. It is a much bigger challenge to obtain improvements in

independent fields. As a typical example we show some changes in the large-scale circulation. The velocity potential shows the large-scale structure of the divergence in the winds and hence the structure of the major overturning cells and the location of convection. At 200 hPa in the December-January-February (DJF) season, there is a global minimum in the velocity potential over the warm pool of the Pacific. This is associated with the divergence in the upper troposphere of rising air due to convection over the warm pool. The global maximum which is associated with sinking air is positioned over the Sahara. In the model both extremes are located too much to the east and are too weak. After optimization, the velocity potential at 200 hPa is closer to Reanalysis data over the Pacific and Indian oceans in the (see Figure 4). The global minimum in the negative cell is positioned closer to New Guinea and has the value $-12 \ 10^6 \ \mathrm{m^2 \ s^{-1}}$ as in the Reanalysis data. The position and value of the local minimum over the North Pacific is also in better agreement with Reanalysis data. The maximum in the positive cell moved from the Middle East to the eastern Sahara. The local minimum and maximum over South America and the eastern Pacific respectively are not present in either the initial or optimized versions of the model. In the June-July-August (JJA) season the velocity potential at 200 hPa has a global minimum over the Philippine Basin in the west Pacific (not shown). The global maximum is positioned over the South Atlantic at 20°S. In SpeedO both these extremes are located too far east. Optimization didn't improve their positions but the value of the maximum (minimum) changed from $+13 \ 10^6 \ \mathrm{m^2 \ s^{-1}}$ ($-14 \ 10^6 \ \mathrm{m^2 \ s^{-1}}$) to $+12 \ 10^6 \ \mathrm{m^2 \ s^{-1}}$ ($-12 \ 10^6 \ \mathrm{m^2 \ s^{-1}}$). The Reanalysis gives maximum and minimum values of $+14 \ 10^6 \ \mathrm{m^2 \ s^{-1}}$ and $-19 \ 10^6 \ \mathrm{m^2 \ s^{-1}}$. So the optimized model is not as good as the original in this season.

11

Initially, the humidity in the troposphere was too high as can be seen in Figure 5a. It was reduced by the optimization by up to 0.5 g kg^{-1} (see Figure 5b). The lower humidity results in a weaker greenhouse trapping. At the same time the temperature of most of the atmosphere was lowered by about 0.5 K (not shown). The cloud top level where most long wave radiation is emitted into space is located mainly in the area with lower temperature. The resulting reduced emission of long wave radiation at the cloud top partially compensates the increased emission at the surface. This explains why after optimization the OLR stays below the climatological value. In several parts of the troposphere the temperature increased by about 0.1 K. This includes the tropics below the 850 hPa and above the 400 hPa level, the Arctic below the 850 hPa level and the Antarctic above the 400 hPa level. The increased temperature gradient between the lower and middle troposphere over the tropics strengthens the Hadley Cells, especially the northern cell, as shown in Figure 6. This means that the subsidence is stronger which causes the drying of the atmosphere.

The precipitation only changed a small amount. The spatial pattern of change matches the errors in the data from the original model compared to CMAP data. The error in the 2 meter air temperature over sea was reduced by almost a factor two in the tropics. However, in the mid-latitudes the error increased a little.

4   Discussion and Conclusions

We have presented a method to efficiently optimize parameters in an AGCM. Our method uses the downhill simplex method to minimize a cost function incorporating mainly TOA

and surface radiation and heat fluxes. Some of the parameters were constrained but none of the optimum parameters values were close to the imposed minimum and/or maximum values. The optimized SpeedO model showed improved radiation budget and large-scale circulation.

In order to test the robustness of the method we have done two tests. First, we restarted optimization with perturbed values of the optimal parameter values. This optimization process resulted in the same optimal values for χ^2 and all parameters within the error tolerance. Second, we have checked the influence of the amount of data used to compute the models climatology after each run by increasing the period over which the model's climatology is computed from 4 to 8 years. In this test χ^2 also converges to the value obtained during the original optimization process. All the parameter values found were close to the original optimal values.

The downhill simplex method can be applied to different components of climate models as well as to coupled models. It imposes no maximum on the number of parameters. However, for very large numbers of parameters $(O(10^3)$ or more) an ensemble Kalman filter will be more efficient. An important advantage of the downhill simplex method is that the cost function can depend in a strongly nonlinear manner on its parameters. This is often the case when optimizing the parameters of a climate model. The method does not require derivatives. As a result, the cost function can have discontinuities. This enables one to incorporate a priori knowledge about valid parameter values in the cost function by setting it to a very large value. Model runs that fail to complete successfully can be dealt with in this manner as well.

A disadvantage of the downhill simplex method is that it is not well suited for parallelization. Only during a contraction step d runs can be done in parallel where d is the number of parameters that are being optimized. In practice, this step is not executed very often. All considering we conclude that the downhill simplex method is a viable approach to finding optimal parameter values for general circulation models that is efficient and easy to use.

References

Annan, J.D., J.C. Hargreaves, N.R. Edwards, and R. Marsh, 2004: Parameter estimation in an intermediate complexity earth system model using an ensemble Kalman filter, *Ocean Modeling*, in press.

Annan, J.D. and J.C. Hargreaves, 2004: Efficient parameter estimation for a highly chaotic system, *Tellus A*, in press.

Bracco, A., F. Kucharski, R. Kallummal, and F. Molteni: Internal variability, external forcing and climate trends in multi-decadal AGCM ensembles. *J. Climate*, submitted.

Da Silva, A.M., C.C. Young, and S. Levitus, 1994: *Atlas of surface marine data 1994*, vol 1, *Algorithms and Procedures, NOAA Atlas 6*, 83 pp. Natl. Oceanic and Atmos. Admin., U.S. Dep. of Commer., Washington, D.C.

Davey, M.K. and coauthors, 2002: STOIC: a study of coupled model climatology and variability in tropical ocean regions, *Clim. Dyn.*, **18**, 403-420.

Hazeleger, W., C. A. Severijns, R. Haarsma, F. Selten, and A. Sterl, 2003: SPEEDO - model description and validation of a flexible coupled model for climate studies, *KNMI, Tech. Rep.*, TR-257, 37 pp.

Kalnay, E. and coauthors, 1996: The NCEP/NCAR 40-year reanalysis project, *Bull. Amer. Meteorol. Soc.*, **77**, 437-471.

Latif, M. et al., 2001: ENSIP: The El Niño Simulation Intercomparison Project. *Clim. Dyn.*, **18**, 255-276.

Molteni, F., 2003: Atmospheric simulations using a GCM with simplified physical parameterizations. I: model climatology and variability in multi-decadal experiments. *Clim. Dyn.*, **20**, 175-191

Oberhuber, J. M., 1988: An atlas based on COADS data set, *Max-Planck-Institut für Meteorologie*, Tech. Rep. 15.

Peixoto, J. P. and A.H. Oort, 1991: Physics of Climate, *American Institute of Physics*, 520 pp.

Press, W. H., S. A. Teukolsky, W. T. Vetterling, B. P. Flannery, 1992: Numerical Recipes in Fortran, 2nd ed., Cambridge University Press, 402-406.

Sennéchael, N., C. Frankignoul, and M. Cane., 1994: An adaptive procedure for tuning a sea surface temperature model, *J. Phys. Oceanogr.*, **24**, 2288-2305

Taylor, P. K., ed., 2000: Final report of the Joint WCRP/SCOR Working Group on Air-Sea Fluxes, Intercomparison and Validation of Ocean-Atmosphere Energy Flux Fields, WMO/TD-No. 1036

Terray, L., 1998: Sensitivity of climate drift to atmospheric physical parameterizations in a coupled ocean-atmosphere general circulation model, *J. Climate*, **11**, 1633-1658

Wahba, G., D. Johnson, F. Gao, and J. Gong, 1995: Adaptive tuning of numerical weather

prediction models: randomized gcv in three- and four-dimensional data assimilation, *Mon. Wea. Rev.*, **123**, 3358-3369

Xie and Arkin, 1996: Analysis of Global Monthly Precipitation Using Gauge Observations, Satellite Estimates, and Numerical Model Predictions, *J. Climate*, **9**, 840-858

Table Captions

Table 1 The data fields included in the reference data set.

Table 2 Global mean energy fluxes before and after optimization. All quantities are in W m^{-2} with positive values indicating upward fluxes. TSR: top solar radiation, SSR: surface solar radiation, SLR: surface long wave radiation, OLR: outgoing long wave radiation, SHF: sensible heat flux, LHF: latent heat flux, NHFS: net heat flux over sea, NHFL: net heat flux over land. The data in the second column are from Peixoto and Oort (1991).

Figure Captions

Figure 1 (a) The cost function χ^2 versus the iteration number for the optimization of the radiation and cloud parameterizations in Speedy with prescribed surface boundary conditions. (b) The value of the parameters RHtop and RHsurf. These are threshold values for cloud formation at the top of the atmosphere and at the surface.

Figure 2 The sea surface solar radiation in SpeedO. (a) and (b) show the annual mean and (c) and (d) the errors compared to Da Silva data. Figures (a) and (c) are for the original model, figures (b) and (d) for the optimized model. Contours are drawn every 25 W m^{-2} in figures (a) and (b) and values above 100 W m^{-2} are shaded. In figures (c) and (d) contours are drawn every 10 W m^{-2} and values above 30 W m^{-2} and below -30 W m^{-2} are shaded.

Figure 3 The latent plus sensible heat flux in SpeedO. (a) and (b) show the annual mean and (c) and (d) the errors compared to Da Silva data. Figures (a) and (c) are for the initial model and (b) and (d) for the optimized mode. Contours are drawn every 25 W m^{-2} in figures (a) and (b) and values above 100 W m^{-2} are shaded. In figures (c) and (d) contours are drawn every 10 W m^{-2} and values above 40 W m^{-2} and below -40 W m^{-2} are shaded.

Figure 4 The mean velocity potential at 200 hPa in the December-January-February (DJF) season in 10^6 m^2 s^{-1}. The top row shows the climatological means and the bottom row the error in the model compared to the Reanalysis. Figures (a) and (c)

are for the initial model, (b) and (d) for the optimized model. Contours are drawn every 10^6 m^2 s^{-1}. Values above 5 10^6 m^2 s^{-1} and below -5 10^6 m^2 s^{-1} are shaded.

Figure 5 The difference in zonal mean specific humidity in g kg^{-1} between the initial SpeedO model and the Reanalysis (a) and the optimized model and the Reanalysis (b). Contours are drawn every 0.1 g kg^{-1} and values above 0.5 g kg^{-1} and below -0.5 g kg^{-1} area shaded.

Figure 6 (a) The meridional overturning in SpeedO before optimization in 10^{10} kg s^{-1}. Values above 5 10^{10} kg s^{-1} and below -5 10^{10} kg s^{-1} are shaded. (b) The change in the meridional overturning as the result of the optimization in 10^{10} kg s^{-1}.

Data field	Source/Value	σ^F
TOA solar radiation	Reanalysis	10 W m^{-2}
TOA long wave radiation	Reanalysis	10 W m^{-2}
Specific humidity at 925 hPa	Reanalysis	0.5 g kg^{-1}
Sea surface solar radiation	Da Silva	10 W m^{-2}
Sea surface long wave radiation	Da Silva	10 W m^{-2}
Sea surface latent heat flux	Da Silva	10 W m^{-2}
Sea surface sensible heat flux	Da Silva	10 W m^{-2}
Zonal mean precipitation	CMAP	0.2 mm day^{-1}
Cloud cover	Oberhuber	10 %
Land heat flux	$\equiv 0$	1 W m^{-2}
Global mean sea heat flux	$\equiv 0$	0.1 W m^{-2}
Global mean e-p budget	$\equiv 0$	0.01 mm day^{-1}

Table 1: The data fields included in the reference data set.

Quantity	Data	Initial	Optimized
TSR	−239	−223.6	−236.3
SSR	−171	−158.6	−168.3
SLR	68	52.69	61.62
OLR	239	223.5	230.7
SHF	20	23.69	21.23
LHF	82	83.38	80.64
NHFS	n.a.	13.79	5.629
NHFL	n.a.	−19.19	−18.39

Table 2: Global mean energy fluxes before and after optimization. All quantities are in W m^{-2} with positive values indicating upward fluxes. TSR: top solar radiation, SSR: surface solar radiation, SLR: surface long wave radiation, OLR: outgoing long wave radiation, SHF: sensible heat flux, LHF: latent heat flux, NHFS: net heat flux over sea, NHFL: net heat flux over land. The data in the second column are from Peixoto and Oort (1991).

(a)   (b)

Figure 1: (a) The cost function χ^2 versus the iteration number for the optimization of
the radiation and cloud parameterizations in Speedy with prescribed surface boundary
conditions. (b) The value of the parameters RHtop and RHsurf. These are threshold
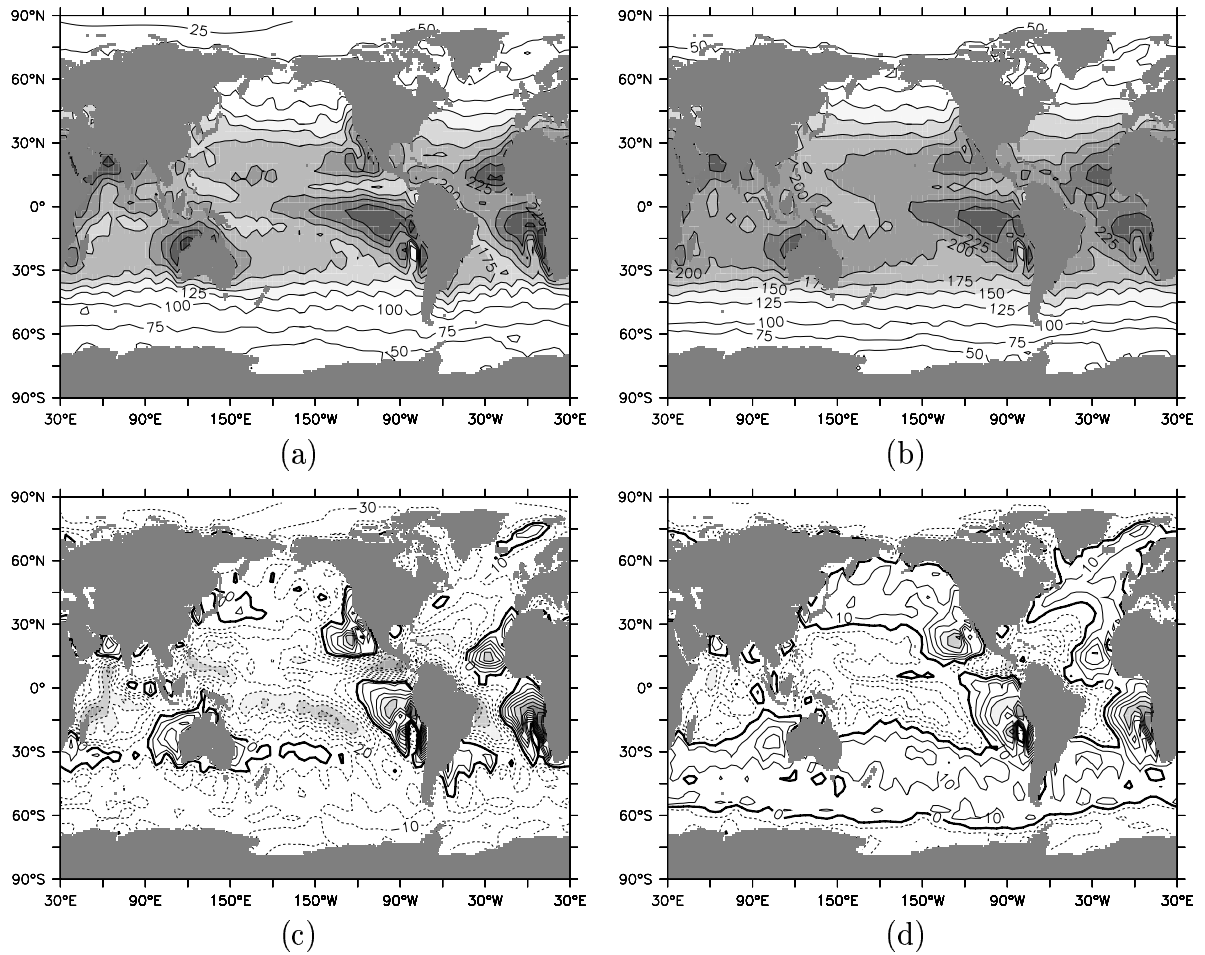values for cloud formation at the top of the atmosphere and at the surface.

Figure 2: The sea surface solar radiation in SpeedO. (a) and (b) show the annual mean and (c) and (d) the errors compared to Da Silva data. Figures (a) and (c) are for the original model, figures (b) and (d) for the optimized model. Contours are drawn every 25 W m^{-2} in figures (a) and (b) and values above 100 W m^{-2} are shaded. In figures (c) and (d) contours are drawn every 10 W m^{-2} and values above 30 W m^{-2} and below -30 W m^{-2} are shaded.
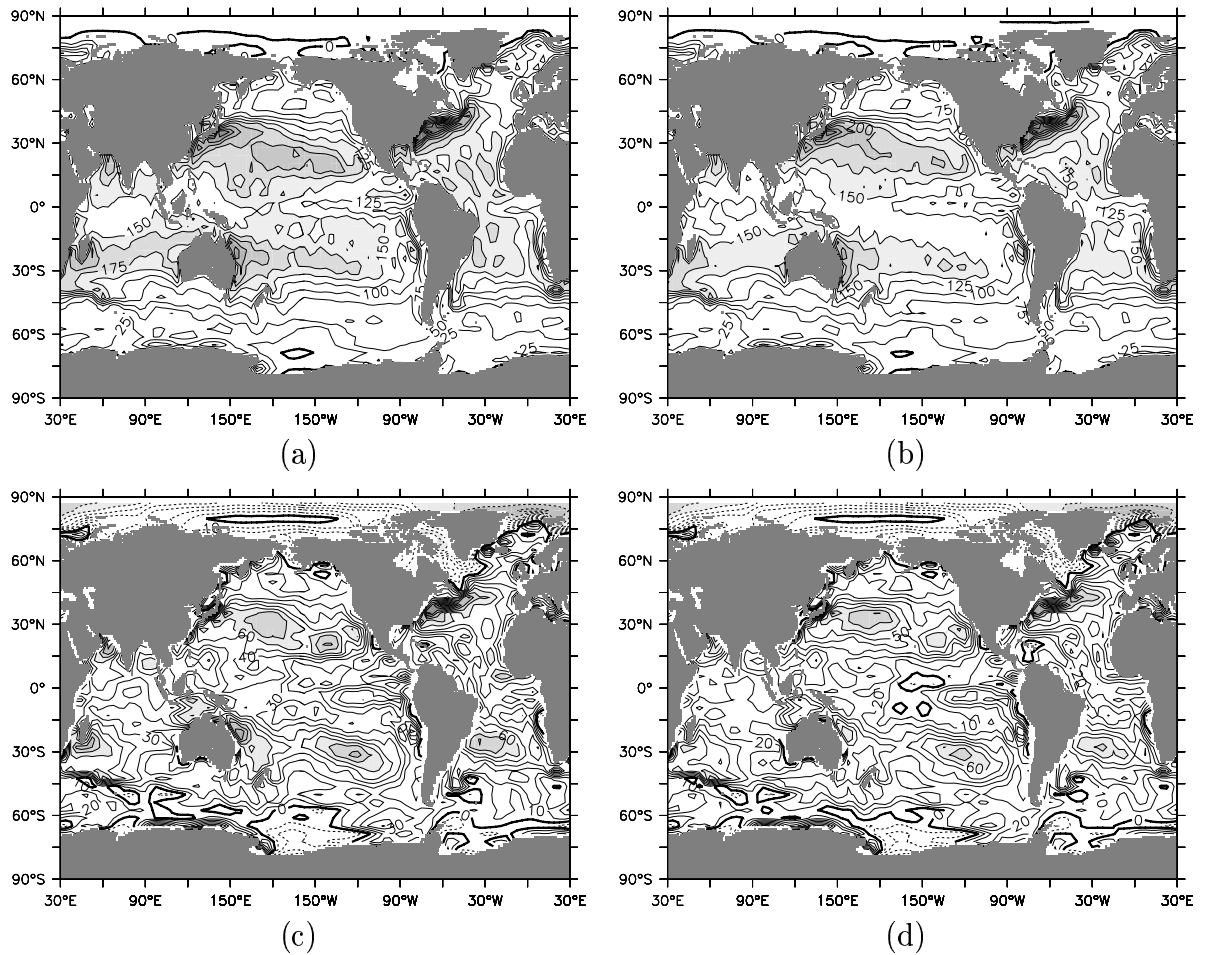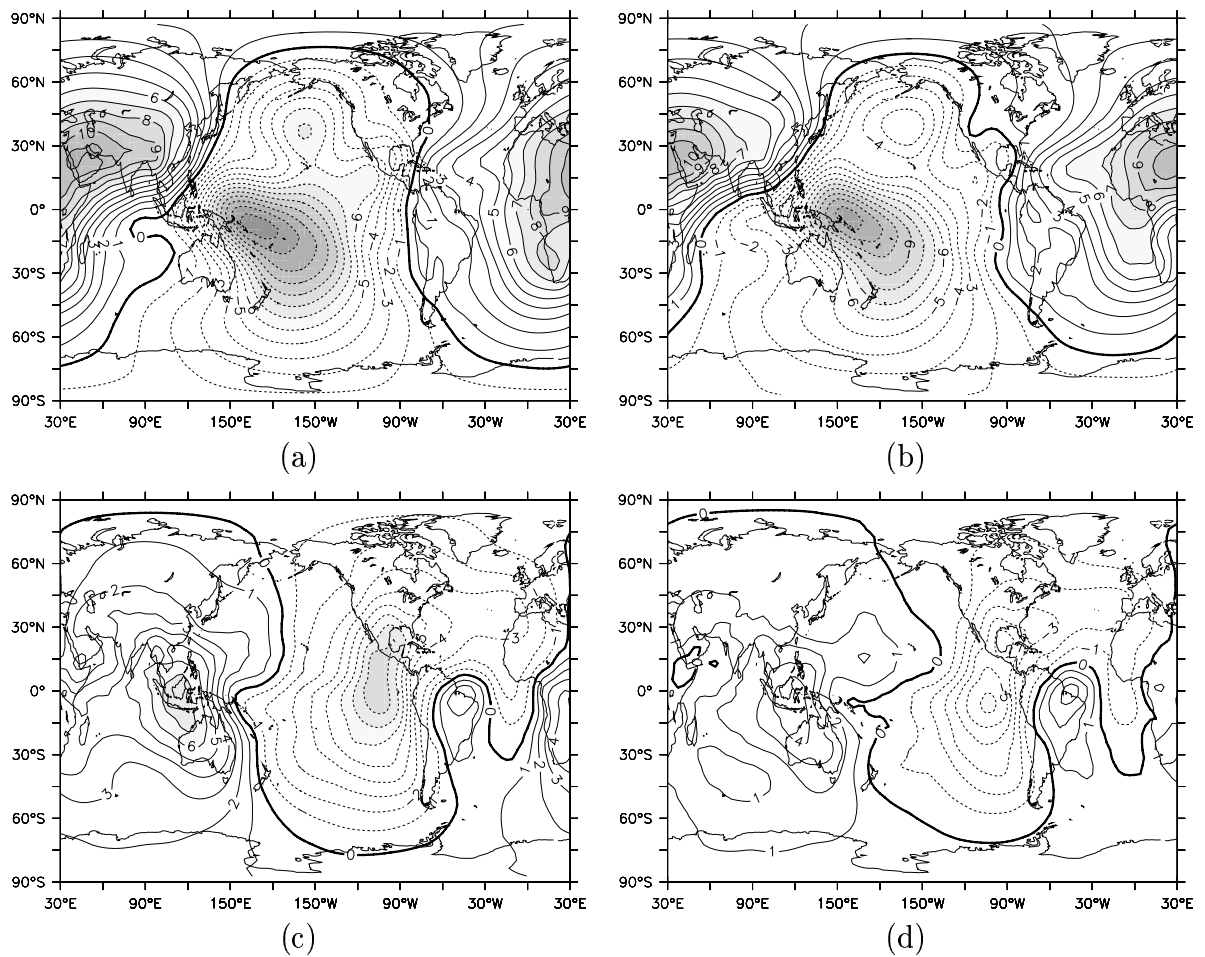
Figure 3: The latent plus sensible heat flux in SpeedO. (a) and (b) show the annual mean and (c) and (d) the errors compared to Da Silva data. Figures (a) and (c) are for the initial model and (b) and (d) for the optimized mode. Contours are drawn every 25 W m^{-2} in figures (a) and (b) and values above 100 W m^{-2} are shaded. In figures (c) and (d) contours are drawn every 10 W m^{-2} and values above 40 W m^{-2} and below -40 W m^{-2} are shaded.

Figure 4: The mean velocity potential at 200 hPa in the December-January-February (DJF) season in 10^6 m^2 s^{-1}. The top row shows the climatological means and the bottom row the error in the model compared to the Reanalysis. Figures (a) and (c) are for the initial model, (b) and (d) for the optimized model. Contours are drawn every 10^6 m^2 s^{-1}. Values above $5\,10^6$ m^2 s^{-1} and below $-5\,10^6$ m^2 s^{-1} are shaded.
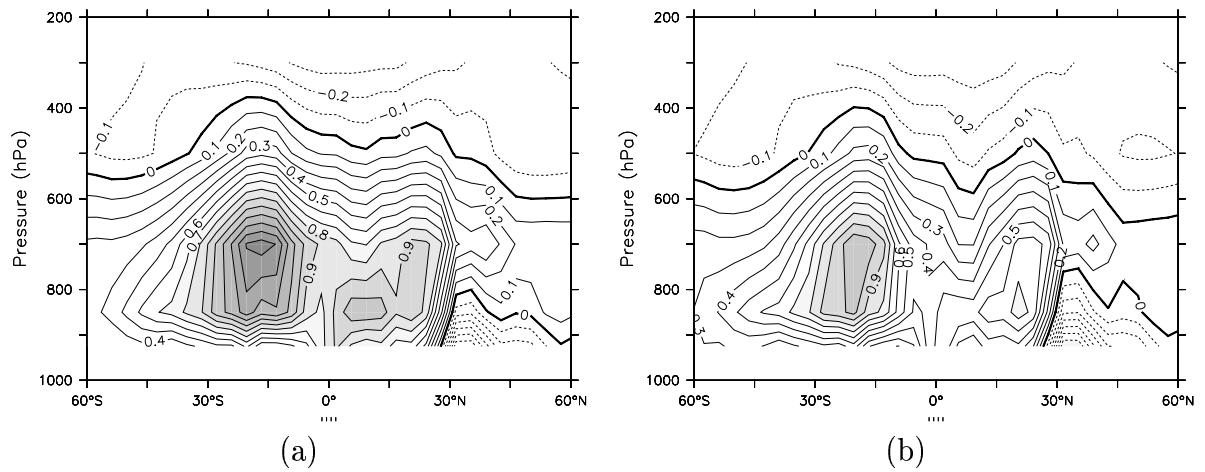
Figure 5: The difference in zonal mean specific humidity in g kg^{-1} between the initial SpeedO model and the Reanalysis (a) and the optimized model and the Reanalysis (b). Contours are drawn every 0.1 g kg^{-1} and values above 0.5 g kg^{-1} and below -0.5 g kg^{-1} area shaded.
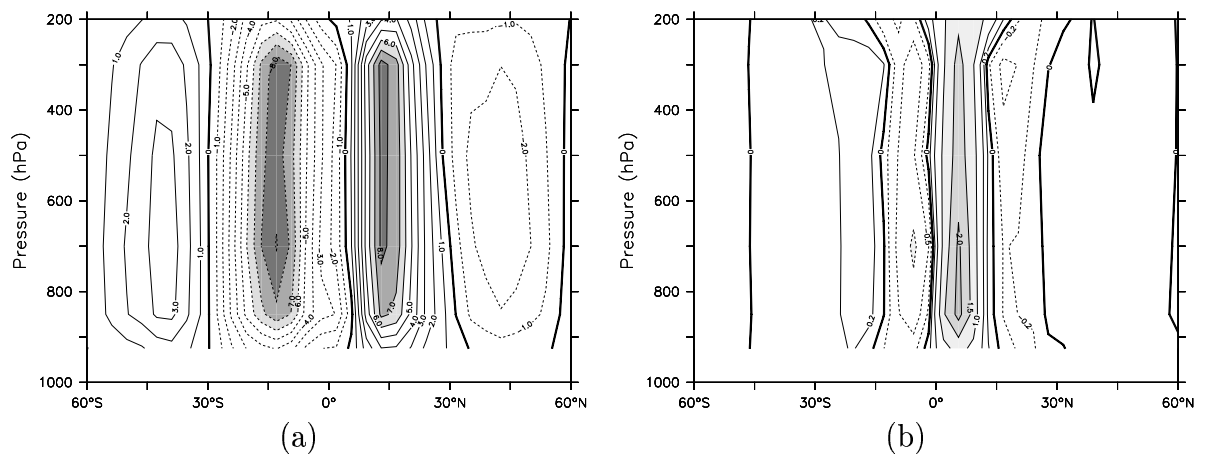
Figure 6: (a) The meridional overturning in SpeedO before optimization in 10^{10} kg s^{-1}. Values above $5 \; 10^{10}$ kg s^{-1} and below $-5 \; 10^{10}$ kg s^{-1} are shaded. (b) The change in the meridional overturning as the result of the optimization in 10^{10} kg s^{-1}.